Available online at www.sciencedirect.com
ScienceDirect
Geochimica et Cosmochimica Acta 74 (2010) 4937–4952
Geochimica et Cosmochimica Acta
www.elsevier.com/locate/gca

Molecular simulation of the diffusion of uranyl carbonate species in aqueous solution

Sebastien Kerisit *, Chongxuan Liu

Pacific Northwest National Laboratory, Chemical and Materials Sciences Division, Richland, WA 99352, USA

Received 9 April 2010; accepted in revised form 2 June 2010; available online 17 June 2010

Abstract

Potential-based molecular dynamics simulations of aqueous uranyl carbonate species ($M_xUO_2(CO_3)_y^{2+2x-2y}$ with M = Mg, Ca, or Sr) were carried out to gain molecular-level insight into the hydration properties of these species. The simulation results were used to estimate the self-diffusion coefficients of these uranyl carbonate species, which often dominate uranyl speciation in groundwater systems. The diffusion coefficients obtained for the monoatomic alkaline-earth cations and polyatomic ions (uranyl, carbonate, and uranyl tri-carbonate) were compared with those calculated from the Stokes–Einstein (SE) equation and its variant formulation by Impey et al. (1983). Our results show that the equation of Impey et al. (1983), originally formulated for monovalent monoatomic ions, can be extended to divalent monoatomic ions, with some success in reproducing the absolute values and the overall trend determined from the molecular dynamics simulations, but not to polyatomic ions, for which the hydration shell is not spherically symmetrical. Despite the quantitative failure of both SE formulations, a plot of the diffusion coefficients of the uranyl carbonate complexes as a function of the inverse of the equivalent spherical radius showed that a general linear dependence is observed for these complexes as expected from the SE equation. The nature of the alkaline-earth cation in the uranyl carbonate complexes was not found to have a significant effect on the ion's diffusion coefficient, which suggests that the use of a single diffusion coefficient for different alkaline-earth uranyl carbonate complexes in microscopic diffusion models is appropriate.

The potential model reproduced well published quantum mechanical and experimental data of $Ca_xUO_2(CO_3)_3^{2x-4}$ and of the individual constituent ions, and therefore is expected to offer reliable predictions of the structure of magnesium and strontium uranyl carbonate aqueous species, for which there is no structural data available to date. In addition, the interatomic distances reported for $Ca_xUO_2(CO_3)_3^{2x-4}$ could help with the refinement of the interpretation of EXAFS data of these species, which is made difficult by the similar uranium-distant carbonate oxygen and uranium–calcium distances.

An analysis of the dynamics of water exchange around the alkaline-earth cations revealed that the presence of the uranyl tri-carbonate molecule has a strong influence on the geometry of the cation's first hydration shell, which, in turn, can considerably affect the water exchange kinetics depending on whether the imposed geometry matches that around the isolated alkaline-earth cation. This result shows that the alkaline-earth uranyl carbonate complexes have distinct water exchange dynamics, which may lead to different reactivities. Finally, significant changes in water residence time were also predicted when replacing carbonate for water ligands in the uranyl coordination shell.

1. INTRODUCTION

Uranium is a major groundwater contaminant at uranium processing and mining sites as a result of intentional and accidental discharges of uranium-containing waste products into subsurface environments. Recent

* Corresponding author. Tel.: +1 509 371 6382; fax: +1 509 371 6354.
E-mail address: sebastien.kerisit@pnl.gov (S. Kerisit).

0016-7037/$ - see front matter © 2010 Elsevier Ltd. All rights reserved.
doi:10.1016/j.gca.2010.06.007

spectroscopic and microscopic studies of contaminated sediments from the US Department of Energy (DOE) Hanford Site have revealed that uranium is present in these sediments as uranyl species [U(VI)] in microscopic intragrain domains (Liu et al., 2004; McKinley et al., 2006). Desorption and diffusion characterizations and numerical modeling indicated that ion diffusion in the micro-porous domains was a major mechanism that led to preferential uranium concentration in the sediment and was predicted to regulate the future release of U(VI) from the contaminated sediment as a long-term source at the site (Liu et al., 2004, 2006b; Ilton et al., 2008). Other studies also implied the importance of diffusion in rate-limiting U(VI) release from contaminated sediments (Braithwaite et al., 1997; Mason et al., 1997; Liu et al., 2008; Stubbs et al., 2009) and related processes of uranyl surface complexation reactions in poorly-connected porous regions (Liu et al., 2009a), uranyl dissolution and precipitation reactions in intragrain weathered fractures (Liu et al., 2006b; McKinley et al., 2006), and microbially-mediated redox reactions in diffusion-controlled domains (Liu et al., 2009b). These experimental and modeling studies collectively indicate that diffusion controls the rates of reactant supply and product removal, thereby affecting the local concentration gradients and chemical compositions, which, in turn, influence further reactions and diffusion, thus leading to a complex coupling between diffusion and geochemical and biogeochemical reactions. However, one important limitation in such characterization and modeling studies is the lack of self-diffusion coefficients for uranyl species in groundwater that are required to interpret experimental results and predict future release rates. This limitation often has forced researchers to adopt empirical approaches in diffusion studies by assuming, for example, that all uranyl species had the same diffusion coefficient (Bai et al., 2009, and references therein), or, by incorporating diffusion coefficients into other effective rate parameters (Liu et al., 2008, 2009a). It is unclear, however, how such empirical treatment of diffusion coefficients affects the local diffusion rates, the rates of geochemical and biogeochemical reactions, and charge and species concentration coupling along diffusion paths.

Although experimental techniques have been developed for determining water and ion self-diffusion coefficients such as the nuclear magnetic resonance spin echoes in the presence of pulsed magnetic field gradients (Stejskal and Tanner, 1965) (PGSE-NMR) or the diaphragm cell technique (Northrop and Anson, 1929), the determination of self-diffusion coefficients for uranyl species is often challenging because of the co-existence of various U(VI) aqueous species under most experimental conditions (Guillaumont et al., 2003). In this regard, the use of molecular simulation techniques provides an attractive alternative method to determine the self-diffusion coefficients of uranyl species.

The overarching goal of this work is to provide an atomic-level characterization of aqueous uranyl carbonate species using molecular simulation with an emphasis on the determination of their self-diffusion coefficients. Molecular dynamics (MD) simulations have been used extensively to calculate the self-diffusion coefficients of ions in aqueous solutions (Impey et al., 1983; Lee and Rasaiah, 1994, 1996; Koneshan et al., 1998) and to assess the physical factors that determine their values (Impey et al., 1983; Møller et al., 2005; Bourg and Sposito, 2007; Bourg et al., 2010). In addition, molecular simulation techniques can address the changes in self-diffusion coefficient of various species in porous media with variable pore sizes and pore surface charges. For example, several research groups have used molecular dynamics techniques to explore the effects of mineral surfaces on water and ion diffusion, including at the surface of clay (Rotenberg et al., 2007; Marry et al., 2008), oxide (Predota et al., 2007), hydroxide (Kalinichev and Kirkpatrick, 2002; Sakuma et al., 2004; Wang et al., 2006), feldspar (Kerisit and Liu, 2009), mica (Wang et al., 2006; Sakuma and Kawamura, 2009), calcium silicate (Kalinichev and Kirkpatrick, 2002; Kalinichev et al., 2007), and carbonate (Kerisit and Parker, 2004) minerals. However, for molecular models to predict diffusion coefficients with a high level of confidence, a thorough evaluation of their performance needs to be carried out first and, accordingly, the second goal of this work is to evaluate the ability of the molecular model constructed in this study for predicting known structural and dynamical properties of uranyl carbonate species and those of their constituent ions.

Uranium(VI) can complex with various inorganic ligands to form aqueous complexes. Uranyl carbonate species, including $Ca_2UO_2(CO_3)_3$ and $CaUO_2(CO_3)_3^{2-}$, will dominate U(VI) aqueous speciation in circumneutral to weakly basic conditions that are representative of Hanford groundwater conditions (Wang et al., 2004). The aqueous complex $Ca_2UO_2(CO_3)_3$ was first reported by Bernhard et al. (1996) from time-resolved laser-induced fluorescence spectroscopy (TRLFS). Studies by Kalmykov and Choppin (2000) and Bernhard et al. (2001) confirmed the formation of the $Ca_2UO_2(CO_3)_3$ complex. Bernhard et al. (2001) also reported extended X-ray absorption fine structure (EXAFS) spectra of uranium L_{II} and L_{III}-edges. Although their results are consistent with the formation of $Ca_2UO_2(CO_3)_3$, the difference between the spectra obtained with and without calcium was not significant due to the almost identical uranium-terminal carbonate oxygen and uranium–calcium distances in the complex. Similar issues were encountered by Kelly et al. (2005, 2007) with uranium L_{III}-edge EXAFS measurements leading to uncertainties on the exact stoichiometry, although the existence of a $Ca_xUO_2(CO_3)_3$ complex was unequivocal. Therefore, molecular simulations can prove to be useful to help determine unambiguously the structure of alkaline-earth uranyl carbonate complexes. Other alkaline-earth uranyl carbonate complexes (namely those formed with Mg^{2+}, Sr^{2+}, and Ba^{2+} ions in addition to Ca^{2+}) have been identified by Dong and Brooks (2006, 2008) using an anion exchange method and by Geipel et al. (2008) on the basis of TRLFS measurements; however, their structures have not been resolved with EXAFS as it has been done for the calcium complexes. Hence, the third goal of this work is to provide structural information regarding alkaline-earth uranyl carbonate species to complement experimentally-derived structures and stoichiometries and to identify any potential trend in the structural and/or dynamical properties of these species when varying the nature of the alkaline-earth cation.

2. COMPUTATIONAL METHODS

2.1. Potential model parameters

In the model used in this work, the atoms of a system are represented as point-charge particles that interact via long-range Coulombic forces and short-range interactions. The latter represent the repulsion between electron-charge clouds, the van der Waals attraction forces, and many-body terms such as bond bending. Several potential models (Guilbaud and Wipff, 1993, 1996; Steele et al., 2000; Greathouse et al., 2002; Druchok et al., 2005; Lins et al., 2008) have been used in MD simulations of UO_2^{2+} with a majority based on the derivation of Guilbaud and Wipff (1993, 1996). Although several models exist for modeling carbonate ions in carbonate minerals (Dove et al., 1992; Pavese et al., 1992, 1996; Catti et al., 1993; Fisler et al., 2000; Archer et al., 2003), few studies report the use of potential models for simulating carbonate ions in aqueous solutions (Greathouse et al., 2002; Kerisit et al., 2005; Bruneval et al., 2007). From the studies referenced above, we assembled a consistent set of potential parameters for modeling alkaline-earth uranyl carbonate species in solution. As it is our intention to use this study as a basis for future work on the interaction of uranyl carbonate species with mineral surfaces, such as feldspar surfaces, for which we have already carried out molecular simulations in the absence of uranyl carbonate species (Kerisit et al., 2008; Kerisit and Liu, 2009), we have chosen to use a potential model which is compatible with that employed in our previous studies. Therefore, our potential model makes use of the extended simple point charge (SPC/E) water model (Berendsen et al., 1987) and is non-polarizable. This will enable us to treat systems large enough to determine the effects of mineral surfaces on the diffusion of uranyl carbonate species in nanosized mineral fractures. The assembled model uses the SPC/E water model (Berendsen et al., 1987), the uranyl potential parameters of Guilbaud and Wipff (1996), the carbonate parameters of Pavese et al. (1996). The carbonate model was transformed from a shell model, as originally described by Pavese et al. (1996), to a non-polarizable model by removing the oxygen shells and assigning the oxygen charge to the core. In addition, potential parameters for modeling the interactions between alkaline-earth cations and both water and carbonate were taken from de Leeuw and Parker (1997) for calcium, de Leeuw and Parker (2000) for magnesium with the modified magnesium–water potential of Kerisit and Parker (2004), and de Leeuw (2002) for strontium with the modified strontium–water potential of Kerisit and Parker (2004). Finally, the potential parameters of Wander et al. (2006), which were used in conjunction with the same carbonate and carbonate–water potentials as used in this work, were employed to describe the uranyl–carbonate ion interactions.

The SPC/E model was selected for consistency with our previous work on water–feldspar interfaces (Kerisit et al., 2008; Kerisit and Liu, 2009), thus allowing us to model the interaction of uranyl carbonate species with feldspar surfaces in the future. The model of Guilbaud and Wipff (1996) was selected as it is one of the most commonly used models for UO_2^{2+}. In addition, this model was derived with the water model TIP3P (Jorgensen et al., 1983), a rigid three-site model similar to SPC/E. The use of the model of Pavese et al. (1996) for the carbonate ion allows us to employ the series of alkaline-earth metal-carbonate potentials that have been developed and evaluated by Parker, de Leeuw and co-workers for a number of years. All the potential parameters and ionic charges used in this work are reported in the Electronic Annex.

2.2. Molecular dynamics simulations

All the calculations were carried out with the computer program DL_POLY (Smith and Forester, 1996), at 298.15 K and zero applied pressure, and in the NPT ensemble (constant number of particles, constant pressure, and constant temperature) for a system of one ion or complex and several hundred water molecules in a cubic box. For charged systems, the net charge was neutralized by a uniform background charge density. The simulation cells contained 506–512 water molecules, depending on the size of the species of interest, which corresponds to box lengths of approximately 25 Å. The geometry of the water molecules was held fixed using the SHAKE algorithm (Ryckaert et al., 1977). The temperature and pressure were kept constant via the use of the Nosé-Hoover thermostat (Hoover, 1985) and the Hoover barostat (Melchionna et al., 1993), respectively. The electrostatic forces were calculated by means of the Ewald summation method (Ewald, 1921). A 9 Å cutoff was used for the short-range interactions and the real part of the Ewald sum. The Ewald sum parameters were chosen to achieve a relative error on the electrostatic energy of at most 10^{-7}. The Verlet leapfrog integration algorithm was used to integrate the equations of motion with a time step of 0.001 ps. All simulations were run for 10,000 ps after an equilibration period of 100 ps. This equilibration time was sufficient for the systems to reach equilibrium. Indeed, using the MD simulation of $Ca_2UO_2(CO_3)_3$ as an example, Figs. A1 and A2 of the Electronic Annex show that the potential energy and pressure of the system have reached their equilibrium value by the end of the equilibration period. The long simulated times of 10,000 ps were required to obtain sufficient statistics for the residence time calculations.

2.3. Self-diffusion coefficients

For each simulation, the self-diffusion coefficient, D, of the species of interest was obtained from its mean square displacement (MSD):

$$Dt = \frac{1}{6}\langle|\mathbf{r}_i(t) - \mathbf{r}_i(0)|^2\rangle \quad (1)$$

where $\mathbf{r}_i(t)$ is the position of atom i at time t. To compute D, a configuration was recorded every 0.2 ps and the ensemble average on the right-hand side of Eq. (1) was calculated over a correlation time of 20 ps. Therefore, the entire MD run was segmented into 20 ps trajectories and each recorded configuration was used as the origin of a new trajectory (for

a total of 49,900 trajectories for each simulation). The correlation time of 20 ps is sufficient for the linear regime to be reached and the gradient of the MSD to be determined, as exemplified in Fig. A3 of the Electronic Annex. The uncertainty on the diffusion coefficient was calculated as the standard deviation of the mean when the trajectories were separated into five blocks. The diffusion coefficients of water, carbonate, and uranyl-containing species were determined from the positions of the oxygen, carbon, and uranium atoms, respectively.

2.4. Residence time calculations

The residence time of water in the hydration shell of the aqueous species, τ, was calculated from the residence-time correlation function (Impey et al., 1983):

$$\langle R(t)\rangle = \left\langle \frac{1}{N_0}\sum_{i=1}^{N_t}\theta_i(0)\theta_i(t)\right\rangle \quad (2)$$

where N_t is the number of water molecules in the first hydration shell at time t and $\theta_i(t)$ is the Heaviside function, which is 1 if the ith water molecule is in the first hydration shell at time t and 0 otherwise. The first hydration shell was considered to extend to the first minimum of the ion–water oxygen radial distribution function. As introduced by Impey et al. (1983), a water molecule was counted as having left the first shell if it has done so for any continuous period of time of at least t^*. This is to allow for water molecules that temporarily leave the first shell and come back without entering the bulk for a significant amount of time to be counted in the residence time. Although Impey et al. (1983) originally used a t^* value of 2.0 ps, subsequent studies (Hofer et al., 2004; Tongraar and Rode, 2005; Laage and Hynes, 2008) identified lower values of t^* as more appropriate and in particular 0.5 ps, which will be used in this work. The residence time can then be obtained by integration of $\langle R(t)\rangle$:

$$\tau = \int_0^\infty \langle R(t)\rangle \, \mathrm{d}t \quad (3)$$

3. RESULTS AND DISCUSSION

3.1. Structural and dynamical hydration properties

We first investigated the hydration properties of the uranyl carbonate species and their constituent ions to evaluate the ability of the potential model to reproduce published quantum mechanical (QM) and experimental data and offer predictions when such data were not available. We focused on: (1) two structural properties: mean interatomic distances (Tables 1–3) and coordination numbers (Tables 1, 2 and 4), both obtained from the relevant radial distribution functions (RDF), and (2) one dynamical property: the residence time of water in the first shell of the ion of interest (Table 5). The two selected structural properties are the most commonly studied and most easily compared with experimental data. Although QM and experimental data are more scarce for the water residence time, this property is of interest to us since it can serve as an indicator of the integrity of the first hydration shell and has been used as a parameter in microscopic conceptual models of ion diffusion (Impey et al., 1983).

For the alkaline-earth and uranyl ions, the mean cation–water oxygen distances and coordination numbers obtained with the potential model are in good agreement with ab initio molecular dynamics simulations and experimental data, as shown in Tables 1 and 2. We note that, because the MD simulations effectively correspond to infinite dilution, we only present, for the calcium, strontium, and uranyl ions, comparison with experimental data obtained with concentrations of 1 M or below in order to reduce the effects of ion pairing as much as possible. The choice of the concentration limit of 1 M was based on the conclusions of Megyes et al. (2006) and Chialvo and Simonson (2003), who showed that for $CaCl_2$ solutions with concentrations of 1 M or less all ions were fully solvated. No concentration limit was imposed for comparison with the MD simulation of magnesium due to the high stability of the $Mg(H_2O)_6^{2+}$ species (Ohtaki and Radnai, 1993). Table 2 also shows that, for the carbonate ion, the potential model predicts a mean hydrogen bond distance between water hydrogen and carbonate oxygen in accord with first-principles MD simulations (Leung et al., 2007; Kumar et al., 2009). However, the coordination numbers of the carbonate oxygen indicate that the potential model predicts one more water of hydration per carbonate oxygen.

Turning to the structure of the uranyl carbonate species, we first note that, to the best of our knowledge, there are no first-principles MD simulations published to date in the literature for these species. Therefore, when comparing with theoretical studies, we contrast our calculated distances with those obtained from QM cluster calculations instead. In addition, in these cases, we have limited ourselves to discussing uranium–carbonate oxygen and uranium–alkaline-earth cation distances, as the distances with water molecules may strongly depend on the extent of hydration. Little data is available for UO_2CO_3 and $UO_2(CO_3)_2^{2-}$. Majumdar et al. (2003) and Majumdar and Balasubramanian (2005) studied the two complexes at three different levels of theory with none or very few waters of hydration and with or without a continuum model of the solvent and found U–$O_{CO_3^{2-}}$ distances varying from 2.193 to 2.360 Å. Kubicki et al. (2009) reported a distance of 2.47 Å for $UO_2(CO_3)_2^{2-}$, obtained at the DFT/B3LYP level of theory with explicit first and second shell water molecules. The distances obtained with the potential model are therefore within the range of published QM cluster calculations. Several theoretical studies that report on the structure of $UO_2(CO_3)_3^{4-}$ have been published. These studies consist in QM cluster calculations with none, one, or two explicit hydration shells treated at various levels of theory (Pyykkö et al., 1994; Hemmingsen et al., 2000; Tsushima et al., 2002; Kubicki et al., 2009). Some of the studies also add a water continuum model (Gagliardi et al., 2001; Vásquez et al., 2003; Austin et al., 2009). The calculated U–$O_{CO_3^{2-}}$ distances vary from 2.41 to 2.60 Å in these studies. EXAFS data revealed distances ranging from 2.42 to 2.44 Å (Bargar et al., 1999;

Table 1
Positions of the first maxima (Å) and coordination numbers (CN) in the radial distribution functions of the alkaline-earth cations as obtained from molecular dynamics simulations at 298.15 K.

Ion	Mg^{2+}		Ca^{2+}		Sr^{2+}	
Property	$M–O_{H_2O}$	CN	$M–O_{H_2O}$	CN	$M–O_{H_2O}$	CN
This work	2.04	6.0	2.36	7.1	2.53	7.7
AIMD	2.13[a]	6.0[a]	2.39[c]	6.0[c]	2.6[e]	7.5[e]
Expt.	2.00–2.15[b]	6.0–6.8[b]	2.42–2.46[d]	6.0–10[d]	2.57–2.65[f]	7.3–10.3[f]

[a] Ikeda et al. (2007b) and Lightstone et al. (2001).
[b] X-ray diffraction (XRD) (Dorosh and Skryshevskii, 1965; Ryss and Radchenko, 1965; Albright, 1972; Caminiti et al., 1977; Caminiti et al., 1979).
[c] Todorova et al. (2008).
[d] XRD (Licheri et al., 1976; Megyes et al., 2004), neutron diffraction (Hewish et al., 1982), and extended X-ray absorption fine structure (EXAFS) spectroscopy (Fulton et al., 2003).
[e] Harris et al. (2003).
[f] EXAFS (Pfund et al., 1994; D'Angelo et al., 1996; Axe et al., 1998; Parkman et al., 1998; Seward et al., 1999; O'Day et al., 2000; Moreau et al., 2002).

Table 2
Positions of the first maxima (Å) and coordination numbers (CN) in the radial distribution functions of the uranyl and carbonate ions as obtained from molecular dynamics simulations at 298.15 K.

Ion	UO_2^{2+}		CO_3^{2-}			
Property	$U–O_{H_2O}$	CN	$O_{CO_3^{2-}}–H_{H_2O}$	CN	$O_{CO_3^{2-}}–O_{H_2O}$	CN
This work	2.48	5.0	1.70	3.9	2.68	4.4
AIMD	2.44–2.49[a]	5.0[a]	1.7–1.8[c,d]	2.8–2.9[c,d]	~2.7[d]	3–3.3[e]
Expt.	2.40–2.46[b]	4.5–5.3[b]	–	–	–	–

[a] Bühl et al. (2006), Frick et al. (2009) and Nichols et al. (2008).
[b] Åberg et al. (1983), Allen et al. (1997), Chisholm-Brause et al. (1994), Hennig et al. (2005), Neuefeind et al. (2004), Sémon et al. (2001), Thompson et al. (1997), and Wahlgren et al. (1999).
[c] Kumar et al. (2009).
[d] Leung et al. (2007).
[e] Rustad et al. (2008).

Table 3
Positions of the first maxima (Å) in the radial distribution functions of the uranyl carbonate and alkaline-earth uranyl carbonate species as obtained from molecular dynamics simulations at 298.15 K.

Species	$U–O_{H_2O}$	$U–O_{CO_3^{2-}}$	U–M	$M–O_{H_2O}$	$M–O_{CO_3^{2-}}$	$O_{CO_3^{2-}}–H_{H_2O}$	$O_{CO_3^{2-}}–O_{H_2O}$
UO_2CO_3	2.49	2.34	–	–	–	1.71	2.69
$UO_2(CO_3)_2^{2-}$	2.49	2.35	–	–	–	1.70	2.68
$UO_2(CO_3)_3^{4-}$	–	2.40	–	–	–	1.69	2.69
$MgUO_2(CO_3)_3^{2-}$	–	2.39	3.74	2.06	2.00	1.69	2.68
$Mg_2UO_2(CO_3)_3$	–	2.38	3.72/4.27	2.05	2.02	1.68	2.66
$CaUO_2(CO_3)_3^{2-}$	–	2.40	4.05	2.38	2.32	1.71	2.70
$Ca_2UO_2(CO_3)_3$	–	2.40	3.99	2.37	2.34	1.71	2.71
$SrUO_2(CO_3)_3^{2-}$	–	2.40	4.10	2.52	2.41	1.69	2.68
$Sr_2UO_2(CO_3)_3$	–	2.40	4.07	2.54	2.41	1.70	2.71

Docrat et al., 1999; Bernhard et al., 2001; Elzinga et al., 2004; Ikeda et al., 2007a). Therefore, the distance predicted by the potential model is only slightly shorter (2.40 Å) than expected from QM cluster calculations and experimental data.

For $Ca_2UO_2(CO_3)_3$, QM cluster calculations at the DFT level of theory with varying numbers of explicit water molecules, and in some cases a water continuum model, resulted in $U–O_{CO_3^{2-}}$ distances from 2.36 to 2.84 Å and U–Ca distances ranging between 3.83 and 4.05 Å (Tsushima et al., 2002; Vásquez et al., 2003; Kubicki et al., 2009). EXAFS data of Bernhard et al. (2001) and Kelly et al. (2007) yielded $U–O_{CO_3^{2-}}$ distances of 2.44 and 2.45 Å, respectively, and U–Ca distances of 3.94 and 4.02 Å, respectively. The $U–O_{CO_3^{2-}}$ distance predicted by the potential model (2.40 Å) is shorter than that obtained with EXAFS but is within the range of published QM calculations. The U–Ca distance (3.99 Å) is in very good agreement with both EXAFS and QM data. All studies referenced above identified the configuration whereby the two calcium ions are in the plane of the

Table 4
Coordination numbers of the uranyl carbonate and alkaline-earth uranyl carbonate species as obtained from molecular dynamics simulations at 298.15 K.

Species	$U–O_{H_2O}$	$U–O_{CO_3^{2-}}$	$M–O_{H_2O}$	$M–O_{CO_3^{2-}}$	$O_{CO_3^{2-}}–H_{H_2O}$	$O_{CO_3^{2-}}–O_{H_2O}$
UO_2CO_3	3.0	2.0	–	–	2.6	3.6
$UO_2(CO_3)_2^{2-}$	1.0	4.0	–	–	2.5	2.6
$UO_2(CO_3)_3^{4-}$	0.0	5.8	–	–	2.6	3.2
$MgUO_2(CO_3)_3^{2-}$	–	6.0	4.0	2.0	2.2	3.2
$Mg_2UO_2(CO_3)_3$	–	6.0	4.5	1.5	1.9	3.4
$CaUO_2(CO_3)_3^{2-}$	–	6.0	4.9	2.0	2.2	2.7
$Ca_2UO_2(CO_3)_3$	–	6.0	5.0	2.0	2.5	2.4
$SrUO_2(CO_3)_3^{2-}$	–	5.9	5.1	2.0	2.2	2.7
$Sr_2UO_2(CO_3)_3$	–	6.0	5.2	2.0	1.8	2.4

Table 5
Water residence time (ps) in the first hydration shell of the alkaline-earth uranyl carbonate species and their constituent ions as obtained from molecular dynamics simulations at 298.15 K. Except for water, the three columns labeled "Oxygen" refer to the residence time of water in the hydration shell of the carbonate oxygens. Additionally, "U + M" corresponds to those carbonate oxygens bound to both uranium and an alkaline-earth cation, "U" to those bound only to uranium, and "free" to those bound to neither.

Species	Cation	Oxygen-free	Oxygen–U	Oxygen–U + M
H_2O	–	4		
Mg^{2+}	>10,000	–	–	–
Ca^{2+}	87	–	–	–
Sr^{2+}	80	–	–	–
UO_2^{2+}	1230	–	–	–
CO_3^{2-}	–	8	–	–
UO_2CO_3	3636	19	17	–
$UO_2(CO_3)_2^{2-}$	7630	21	21	–
$UO_2(CO_3)_3^{4-}$	–	15	15	–
$MgUO_2(CO_3)_3^{2-}$	>10,000	22	18	456
$Mg_2UO_2(CO_3)_3$	>10,000	30	19	404
$CaUO_2(CO_3)_3^{2-}$	476	26	17	47
$Ca_2UO_2(CO_3)_3$	523	43	23	85
$SrUO_2(CO_3)_3^{2-}$	107	20	18	16
$Sr_2UO_2(CO_3)_3$	120	28	24	22

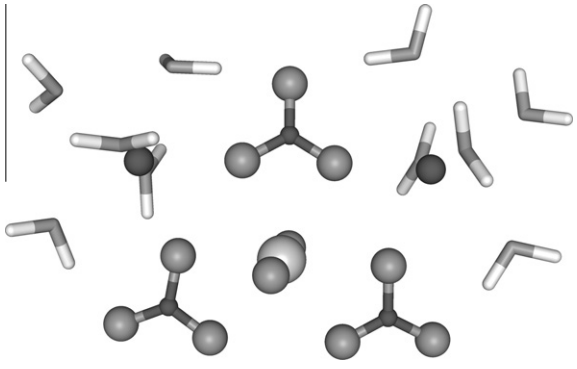

Fig. 1. Snapshot of the aqueous $Ca_2UO_2(CO_3)_3$ complex with first hydration shell of both calcium ions, as obtained from a molecular dynamics simulation at 298.15 K. Oxygen ions are shown in gray, calcium and carbon in dark gray, uranium in light gray, and hydrogen.

carbonate ions and bound to two oxygen atoms from two different carbonate ions as the most probable configuration and, indeed, this is the configuration also obtained with the potential model, as illustrated in Fig. 1 with a snapshot from the MD simulation.

To the best of our knowledge, there is no published data on the structure of magnesium and strontium uranyl tri-carbonate aqueous complexes. However, given the satisfactory description of the structural characteristics of the species for which data is available, the MD simulation results can be used as prediction. The structure of $Sr_xUO_2(CO_3)_3^{2x-4}$ is similar to that of $Ca_2UO_2(CO_3)_3$ with slightly longer $Sr–O_{CO_3^{2-}}$ bond distances, which translate into longer Sr–U distances. $MgUO_2(CO_3)_3^{2-}$ adopts the same configuration as its calcium and strontium counterparts; however, in the simulation of $Mg_2UO_2(CO_3)_3$, one of the two magnesium ions moved so as to incorporate an addition water molecule in its first coordination shell, thereby reducing its coordination number with carbonate oxygens, and remained in this monodentate configuration for the entire MD run. The strong magnesium–water interaction, as exemplified by its slow rate of water exchange relative to calcium and strontium (cf. next paragraph), likely made this exchange possible. In addition, the slow dynamics of water exchange around magnesium on the timescale of the MD simulations also explain why the magnesium ion remained in this configuration for the entire MD run.

For the dynamical properties of the aqueous species, we computed the residence time of water molecules in the first hydration shell of the cations and of the carbonate oxygen atoms, where relevant. The results are summarized in Table 5. Little experimental data is available for comparison. For the alkaline-earth cations, some experimental data are available for Mg^{2+} and Ca^{2+}. Although the residence time of water in the magnesium hydration shell is longer than the timescale of the simulation and therefore no exchange was observed during the entire MD run, previous work (Kerisit and Parker, 2004) using constrained MD simulations and the same magnesium–water potential as used in this work, albeit with a different water model, gave excellent agreement with the experimental data of Bleuzen et al. (1997) ($6.7 \pm 0.2 \times 10^5\ s^{-1}$) and Neely and Connick (1970) ($5.3 \pm 0.3 \times 10^5\ s^{-1}$). For calcium, a quasi-elastic neutron scattering (QENS) study (Salmon et al., 1987) reported a water residence time of less than 100 ps. Also, Schwenk

et al. (2001), who used quantum mechanical/molecular mechanical (QM/MM) MD at the Hartree–Fock and DFT levels, and Naor et al. (2003), who used Car-Parrinello molecular dynamics with the BLYP functional, found that the water residence time in the first hydration shell was on the order of 10 ps. The height of the first maximum of the cation–water oxygen radial distribution function is related to the depth of the free energy well associated with the first hydration shell and therefore is also correlated to the residence time. The value of the RDF at the first maximum was calculated to be 9.4, which compares well with the value of approximately 8 obtained in two first-principles molecular dynamics simulations in which the calcium coordination number was the same as that obtained in our MD simulation, (Naor et al., 2003; Lightstone et al., 2005). This observation further suggests that the dynamics of water exchange around calcium are well described. No experimental data is available for strontium to the best of our knowledge; however, QM/MM MD simulations of Hofer et al. (2006) yielded a residence time of 45 ps and Harris et al. (2003) estimated, from their ab initio molecular dynamics simulation, the water residence time to be on the order of 10 ps. Therefore, we conclude that the dynamics of water around the alkaline-earth cations as predicted by the potential model are consistent with available experimental and QM data.

For the uranyl ion, Grenthe and co-workers (Szabó et al., 1996; Farkas et al., 2000) obtained water exchange rate constants of $1.4 \times 10^6\ s^{-1}$ and subsequently $1.30 \pm 0.05 \times 10^6\ s^{-1}$ from ^{17}O NMR experiments. Consequently, the experimental values suggest that the activation free energy for water exchange is underestimated by the potential model, which predicts an exchange rate of $8.1 \times 10^8\ s^{-1}$. Indeed, the experimentally-derived activation free energy is 38 kJ mol^{-1} (Farkas et al., 2000), whereas that calculated by the potential model is approximately 23 kJ mol^{-1}. Although the uranyl-water potential was derived by Guilbaud and Wipff (1996) to reproduce the hydration free energy of the uranyl ion (relative to that of strontium), it does not give an accurate estimate of the energetics of water exchange. However, the difference between the experimental and calculated activation free energies (~15 kJ mol^{-1}) is similar to the range of activation free energies computed with various electronic structure methods (Vallet et al., 2001; Bühl et al., 2005; Bühl and Kabrede, 2006; Rotzinger, 2007; Wåhlin et al., 2008). This comparison highlights the difficultly in reliably estimating water exchange rates for slow exchanges as small changes in the activation free energy translate into large changes in water exchange rates.

An interesting phenomenon is revealed in Table 5 whereby the residence time of water around calcium in the uranyl carbonate complexes is significantly increased relative to that around the monoatomic cation, whereas for strontium the increase is only slight. We explain this difference by comparing the average first hydration shell geometry of the monoatomic cation to that imposed by the presence of the uranyl tri-carbonate molecule, when the same cation is part of the complex. For calcium, the most probable coordination number calculated from the simulation of the monoatomic cation is 7 (6 = 10%, 7 = 73%, and 8 = 17%) and corresponds to pentagonal bipyramid geometry. As shown in Figs. 1 and 2, replacing two equatorial water molecules with oxygen ions from two carbonate molecules does not significantly disturb this geometry, whereby the $O_{CO_3^{2-}} - Ca - O_{CO_3^{2-}}$ angle is similar to the O_{H_2O}–Ca–O_{H_2O} angle and the axial water molecules are not disrupted by the presence of the uranyl tri-carbonate molecule. In addition, little displacement is necessary for two water molecules to donate a hydrogen bond to two distant carbonate oxygen ions and the geometry thus imposed is symmetrical. Accordingly, the calcium most probable coordination number with water in the complex is 5 (in about 96% of the configurations recorded). For strontium, however, the most probable coordination number calculated from the simulation of the monoatomic cation is 8 (7 = 25.5%, 8 = 72.5%, and 9 = 2%) and corresponds to square antiprism geometry. By contrast, the most probable coordination number with water in the complex is 5 (76%) with a fair proportion of configurations for which CN = 6 (20%). This phenomenon is illustrated in Fig. 2, whereby the densities of the uranium, carbon, carbonate oxygen, alkaline earth, and first shell water oxygen atoms are projected onto the plane formed by the alkaline-earth cation and the two carbonate oxygens it is bound to. The configurations used to generate this figure have been superimposed by using the alkaline-earth cation as origin and aligning the vector formed by the alkaline-earth and uranium atoms with the *x*-axis. Fig. 2 clearly shows the pentagonal bipyramid geometry of the alkaline-earth cation's coordination shell when in the complex and the more diffuse density of the waters of hydration for strontium, in particular for those directly above and below the alkaline-earth cation, which reflects less strongly bound water molecules. This result highlights the importance of the "natural" versus "imposed" geometries of the first hydration shell in determining the kinetics of water exchange around the alkaline-earth cations. Similar concepts have been reported in the inorganic chemistry literature. In particular, van Eldik and co-workers (Schneppensieper et al., 2001) have shown that the rates of water exchange of seven-coordinate aqua-polyaminecarboxylate iron(III) complexes are higher than that of the hexaaqua iron(III) species and they suggested that the increase in water lability could be due to the change in coordination number from 6 to 7 with respect to the fully hydrated species. Similarly, in another study, van Eldik and co-workers (Maigut et al., 2008) demonstrated that the strong preference of nickel(II) for an octahedral coordination gave rise to a different change in water exchange behavior upon complexation by polyaminecarboxylate chelates compared to iron(II), iron(III), and manganese(II), for which sevenfold coordination was possible.

Table 5 also shows that the residence time of water in the first coordination shell of uranium increases as the number of carbonate ligand increases. A radial distribution function analysis of the water and carbonate oxygens in the first hydration shell of uranium of the $UO_2(CO_3)_x(H_2O)_{5-2x}^{2-2x}$ species shows that the mean water oxygen–water oxygen distance increases from 2.92 to 2.97 Å when *x* increases from 0 to 1 and that the mean water oxygen–carbonate oxygen distance increases from 3.10 to 3.19 Å when *x* increases from 1 to 2 (Fig. 3). Therefore, although

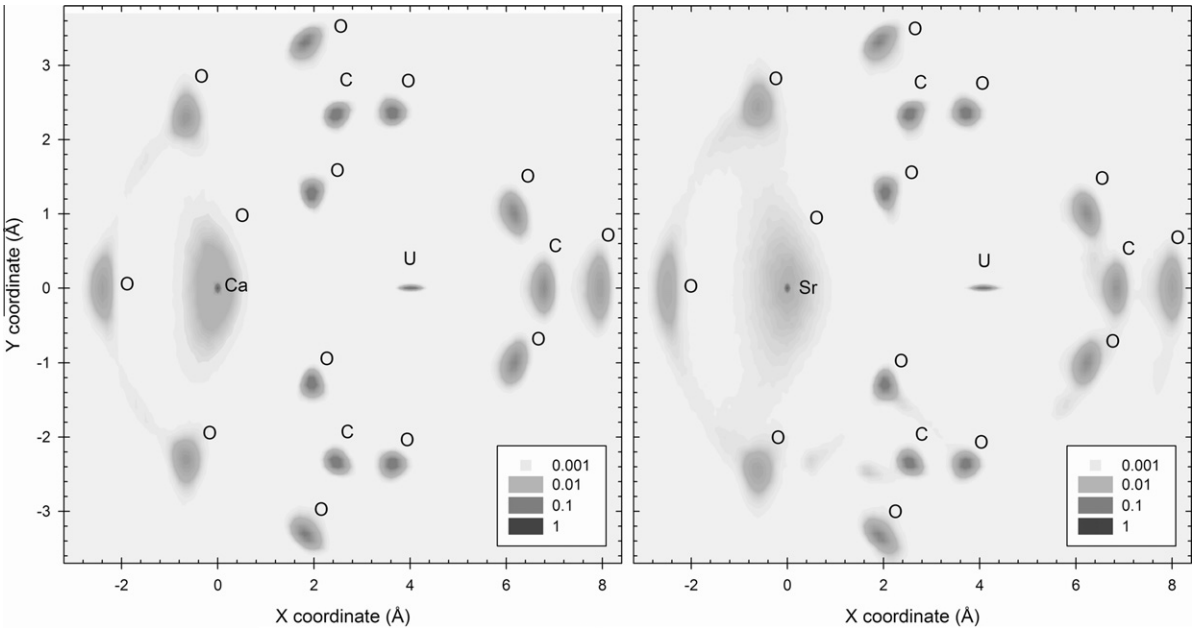

Fig. 2. Uranium, carbon, carbonate oxygen, alkaline-earth, and first shell water oxygen atomic densities as obtained from the molecular dynamics simulations of the $CaUO_2(CO_3)_3^{2-}$ (left) and $SrUO_2(CO_3)_3^{2-}$ (right) species and projected onto the plane formed by the alkaline-earth cation and the two carbonate oxygens it is bound to.

the U – O_{H_2O} distance does not change significantly with the number of carbonate ligands (Tables 2 and 3), the replacement of water ligands by carbonate ions creates more room in the first coordination shell and thus reduces the ligand–ligand repulsion, leading to a decrease in water exchange rate. The changes in water exchange rates upon substitution of stable ligands for water molecules have been well documented in the geochemistry and inorganic chemistry literature (e.g. Kruse and Taube, 1961; Phillips et al., 1997a,b; Phillips et al., 1998; Clark et al., 1999; Helm and Merbach, 2005).

An analysis of the residence time of water in the first shell of carbonate oxygens shows that the residence time is increased by a factor of two when the carbonate ion is bound to the uranyl ion. The rotation of the carbonate molecule is impeded by its coordination to the uranyl ion which increases the residence time of water around oxygen ions. Indeed, a MD simulation of a frozen carbonate molecule in pure water shows an increase in residence time to 29 ps. In the alkaline-earth uranyl carbonate complexes, the residence time of water is increased for those water molecules that are simultaneously in the hydration shell of both the alkaline-earth cation and a carbonate oxygen.

In summary, although a series of molecular dynamics studies on uranyl carbonate species in aqueous solutions in contact with mineral surfaces has been published by Greathouse and co-workers (Greathouse et al., 2002; Greathouse and Cygan, 2005, 2006), this work represents the first detailed characterization of the hydration properties of alkaline-earth uranyl carbonate complexes using molecular dynamics simulations. The main advantages of such simulations are the ability to consider hundreds of water molecules and the capacity for directly probing the kinetics of water exchange over tens of nanoseconds. These unique features of molecular dynamics simulations allowed us to bring to light the influence of the uranyl tri-carbonate molecule on the structure and dynamics of the alkaline-earth cations' hydration shell and vice-versa.

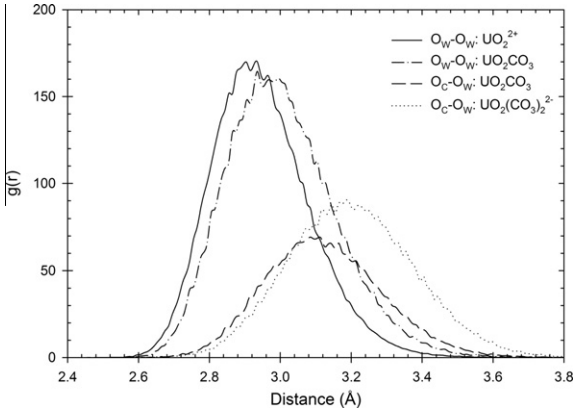

Fig. 3. Radial distribution functions computed using the water oxygen (O_W) and carbonate oxygen (O_C) positions in the uranyl equatorial coordination shell.

3.2. Water diffusion

It has been shown (Dünweg and Kremer, 1991, 1993; Yeh and Hummer, 2004) that long-range interactions in molecular dynamics simulations can significantly affect the calculated self-diffusion coefficient of water due to the limited size of the simulation cells. Indeed, for cubic simulation cells, water self-diffusion coefficient is dependent on $1/L$ where L is the simulation box length. The size-independent self-diffusion coefficient, D_0, is given by:

$$D_0 = D_{PBC} + 2.837297 k_B T/(6\pi\eta L) \quad (4)$$

where D_{PBC} is the diffusion coefficient obtained with the simulation of box length L, η is the water shear viscosity, k_B is Boltzmann constant and T is the temperature. The shear viscosity of the water model of interest can be obtained with molecular dynamics simulations via several methods (Hess, 2002). In this work, we used the fact that Eq. (4) has been well demonstrated and therefore we carried out several simulations with varying box lengths to extract η. Fig. 4 shows the diffusion coefficient of water as a function of box size for the SPC/E water model. As expected a linear dependence of the diffusion coefficient on the inverse of the simulation box length is calculated. The shear viscosity thus extracted is 7.3×10^{-4} kg m^{-1} s^{-1} and the size-independent diffusion coefficient is 2.84×10^{-9} m^2 s^{-1}. The experimental viscosity (2010) is 8.90×10^{-4} kg m^{-1} s^{-1}. Although a range of experimental diffusion coefficients has been reported in the literature, a generally accepted value is 2.3×10^{-9} m^2 s^{-1} (Mills, 1973). Therefore, the low shear viscosity of the SPC/E water model is consistent with its higher diffusion coefficient. Since the water viscosity will affect the prediction of the diffusion coefficients of the uranyl carbonate species, the difference between the experimental and calculated values needs to be taken into account. Therefore, the approach taken hereafter is to normalize all computed diffusion coefficients to the water diffusion coefficient of the SPC/E model. Similarly, experimental diffusion coefficients are normalized to the experimental water diffusion coefficient for comparison.

3.3. Alkaline-earth cation diffusion

We now focus on three alkaline-earth cations, namely, Mg^{2+}, Ca^{2+}, and Sr^{2+}, which are constituent ions of the uranyl carbonate species of interest. In addition, these cations are monoatomic and spherical, which allows us to test the effectiveness of the Stokes–Einstein equation or the modification introduced by Impey et al. (1983) to rationalize the diffusion coefficient. The Stokes–Einstein relation

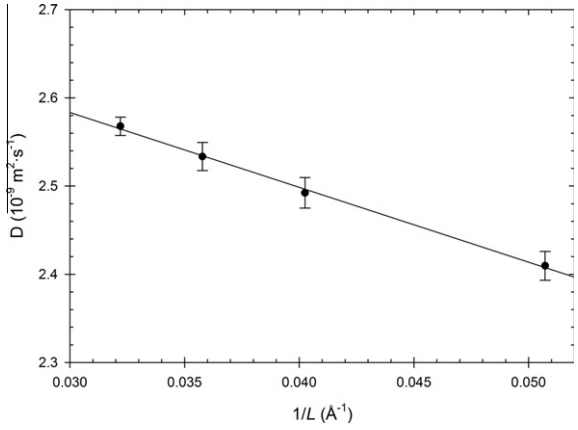

Fig. 4. Water self-diffusion coefficient as a function of the inverse of the simulation cell length obtained with the SPC/E water model.

applies to a spherical molecule of radius R diffusing in a continuum solvent of viscosity η:

$$D = \frac{k_B T}{C\pi\eta R} \quad (5)$$

where two limiting cases exist, which are termed "stick" and "slip" conditions and for which C is 6 and 4, respectively. Therefore, for monoatomic ions, this relationship predicts that the diffusion coefficient decreases linearly with increasing atomic radius. However, this trend is not observed experimentally (Impey et al., 1983). One complication is that the cation–water interactions result in the formation of a hydration shell which moves with the cation and makes the cation effectively larger, thereby slowing down the ion with respect to the predicted diffusion coefficient based on the bare ion radius. This conceptual model is referred to as the solventberg picture. However, the hydration shell is not fully rigid and water molecules can exchange between the first and second hydration shells. Therefore, Impey et al. (1983) introduced a conceptual model to rationalize the observed changes in diffusion coefficient for a series of monovalent monoatomic ions. In this model, an ion of (bare) radius R_I diffuses in a non-uniform solvent whereby the solvent viscosity is distance dependent, meaning that above a cutoff, R_C, the shear viscosity is that of bulk water and within this cutoff distance the viscosity depends on the dynamical properties of the first shell water molecules. This model translates into the following equation, which interpolates between bare slip and fully hydrated stick conditions:

$$D = \frac{k_B T}{4\pi\eta R_I}\left[\frac{\tau^R_{bulk}}{\tau^R_{ion}} + \frac{2R_I}{3R_C}\left(1 - \frac{\tau^R_{bulk}}{\tau^R_{ion}}\right)\right] \quad (6)$$

where τ^R_{bulk} and τ^R_{ion} are the reorientation times of the water molecular dipole axis in the bulk and in the first hydration shell, respectively. Impey et al. (1983) also showed that this ratio is the same as the ratio of the residence time of water in the first hydration shell of the ion and in the bulk.

Therefore, we calculated the alkaline-earth cation diffusion coefficients from (a) molecular dynamics simulations ("calc." column in Table 6); (b) from Eq. (5) with slip conditions and the bare ion radius ("SE-bare" column); (c) from Eq. (5) with stick conditions and the fully hydrated ion radius ("SE-full" column); and (d) from Eq. (6) ("SE-Impey" column). The normalized diffusion coefficients are presented in Table 6 together with available experimental data. The bare and hydrated ion radii were calculated using the approach described by Impey et al. (1983), whereby the bare ion radius is obtained from the mean cation–water oxygen distance minus half the mean oxygen–oxygen distance in bulk water and the hydrated ion radius is obtained from the mean cation–water hydrogen distance plus the hydrogen radius (0.5 Å as used by Impey et al.). As expected, the Stokes–Einstein relationship for bare slip conditions greatly overestimates the diffusion coefficient for all species. Although some improvement is observed for fully hydrated stick conditions, there remain errors as high as 20% and the trend down the periodic table is not reproduced. The diffusion coefficients obtained using Eq. (6)

are more satisfactory with errors of approximately 5% and the correct trend being reproduced. For magnesium, for which no water exchange took place in the first hydration shell, no significant improvement was obtained when considering the second hydration shell, as shown in Table 6.

In conclusion, the conceptual model of Impey et al. (1983) yields satisfactory predictions when extended from its original development for monovalent ions to the divalent cations considered in this study. Importantly, the general experimental trend is reproduced by the potential model, although the difference between the calcium and strontium diffusion coefficients is much greater in the molecular simulations.

3.4. Uranyl diffusion

There is some discrepancy in the literature as to the experimental value of the uranyl self-diffusion coefficient. Early work by Brown et al. (1954a) on the electrical conductivity of uranyl fluoride aqueous solutions resulted in a limiting ionic conductance (i.e., the conductance extrapolated to zero concentration) of 32 cm^2 S val^{-1}, which corresponds to a limiting diffusion coefficient of 0.426×10^{-9} m^2 s^{-1}; however, a study of the conductivity of uranyl sulfate solutions by the same group (Brown et al., 1954b) reported a higher limiting ionic conductance of 51 cm^2 S val^{-1} (i.e., a limiting diffusion coefficient of 0.679×10^{-9} m^2 s^{-1}). In addition, Marx and Bischoff (1976) obtained, using the radioisotope method, a limiting ionic conductance of 57 cm^2 S val^{-1}, which translates into a limiting diffusion coefficient of 0.759×10^{-9} m^2 s^{-1}. As noted by Marx and Bischoff (1976) a value of 57 cm^2 S val^{-1} is consistent with other divalent cations, which by and large vary from 53 to 70 cm^2 S val^{-1}. A study by Kern and Orlemann (1949) reports a diffusion coefficient of 0.68×10^{-9} m^2 s^{-1} in 0.09 M $NaClO_4$ 0.01 M $HClO_4$. This study also reports a diffusion coefficient obtained by Kolthoff and Harris of 0.62×10^{-9} m^2 s^{-1} in 0.1 M KCl 0.01 M HCl. Awakura et al. (1987) measured the diffusion coefficient of U(VI) in uranyl sulfate solutions. Although they did not extrapolate their findings to infinite dilution at zero ionic strength, the trends they observed in the change in diffusion coefficient with uranyl and sulfate concentrations indicate a self-diffusion coefficient greater than that obtained by Brown et al. (1954a). Finally, a theoretical study by Mauerhofer et al. (2004) predicted a diffusion coefficient of 0.779×10^{-9} m^2 s^{-1} based on a geometric model and the microscopic version of the Stokes–Einstein equation. The value of Marx and Bischoff (1976) (0.759×10^{-9} m^2 s^{-1}), being the most recent experimental value explicitly quoted as limiting diffusion coefficient (i.e., the diffusion coefficient extrapolated to zero concentration), is used for comparison in this work. This diffusion coefficient normalized to water diffusion (2.3×10^{-9} m^2 s^{-1}) is therefore 0.330. The potential model gives 0.333 in very good agreement with the experimental data of Marx and Bischoff (1976), thus providing further evidence that the value derived by Brown et al. (1954a), 0.426×10^{-9} m^2 s^{-1}, is in error. It should be noted that, in their paper, Brown et al. (1954a) did caution the reader that their data were corrected for the presence of hydrogen ions but not for other possible ions. Importantly, we note that this value was subsequently tabulated in the CRC Handbook of Chemistry and Physics (Vanysek, 2010) and in a paper by Li and Gregory (Li and Gregory, 1974). A literature search revealed that many studies have used the value of Brown et al. as reported by Li and Gregory (Chaillou et al., 2002, 2008; Zheng et al., 2002; McManus et al., 2005; Liu et al., 2006a; Swarzenski and Baskaran, 2007).

3.5. Uranyl carbonate and alkaline-earth uranyl carbonate diffusion

In this section, we first compare the diffusion coefficients of the uranyl, carbonate, and uranyl tri-carbonate species calculated from the MD simulations with the three versions of the Stokes–Einstein model, as shown in Table 6. The approach taken here was the same as described above with the exception of the calculation of R_I and R_C for anions. As described by Impey et al. (1983), the bare anion radius is obtained from the first peak of the anion–water hydrogen RDF minus the hydrogen radius and the hydrated anion radius is obtained from the second peak of the anion–water hydrogen RDF plus the hydrogen radius. The central atom of the anion of interest (i.e., C or U) was used for computing the anion–water hydrogen RDF. Table 6 shows that, as before, the calculated values are bracketed by those determined from the bare slip and full hydrated stick conditions. However, for these three ions the conceptual model of Impey et al. fails to improve upon the predicted diffusion coefficients. This is most likely due to the fact that the three ions considered here do not adopt a spherical hydration shell. In addition, different regions of the hydration shell can show different dynamics of water exchange as, for example, around the uranyl ion. Consequently, our results show that

Table 6
D_i/D_{H_2O} ratio obtained for $i = Mg^{2+}$, Ca^{2+}, Sr^{2+}, UO_2^{2+}, CO_3^{2-}, and $UO_2(CO_3)_3^{4-}$ from molecular dynamics simulations at 298.15 K. The MD results are compared with experimental data and predictions obtained with the three versions of the Stokes–Einstein (SE) equation, as described in the text.

Species	Calc.	SE-bare	SE-full	SE-Impey	Expt.
Mg^{2+} – 1st shell	0.310	2.386	0.327	0.327	0.307
Mg^{2+} – 2nd shell	0.310	0.552	0.198	0.323	0.307
Ca^{2+}	0.376	1.609	0.298	0.358	0.345
Sr^{2+}	0.359	1.372	0.286	0.340	0.344
UO_2^{2+}	0.333	1.434	0.287	0.290	0.330
CO_3^{2-}	0.353	0.800	0.233	0.517	–
$UO_2(CO_3)_3^{4-}$	0.242	0.524	0.187	0.277	–

Table 7
D_i/D_{H_2O} ratio of the uranyl carbonate and alkaline-earth uranyl carbonate species obtained from molecular dynamics simulations at 298.15 K.

Species	D_i/D_{H_2O}
UO_2CO_3	0.29 ± 0.03
$UO_2(CO_3)_2^{2-}$	0.24 ± 0.03
$UO_2(CO_3)_3^{4-}$	0.24 ± 0.03
$MgUO_2(CO_3)_3^{2-}$	0.22 ± 0.02
$CaUO_2(CO_3)_3^{2-}$	0.22 ± 0.03
$SrUO_2(CO_3)_3^{2-}$	0.21 ± 0.02
$Mg_2UO_2(CO_3)_3$	0.20 ± 0.02
$Ca_2UO_2(CO_3)_3$	0.20 ± 0.02
$Sr_2UO_2(CO_3)_3$	0.21 ± 0.02

the model of Impey et al. can be extended to monoatomic divalent cations but not to polyatomic ions.

Table 7 shows the diffusion coefficients of a series of uranyl carbonate and alkaline-earth uranyl carbonate species obtained from the molecular dynamics simulations. Fig. 5 shows the same data but as a function of the inverse of the equivalent spherical radius of the fully hydrated ion, which was obtained as follows: the molecular volumes of the uranyl and tri-carbonate uranyl ions were calculated using an ellipsoid of revolution with a transverse radius set to the uranium hydrated radius and a conjugate radius set to $d(U–O_{UO_2^{2+}}) + d(O_{UO_2^{2+}}–O_{H_2O}) - d(O_{H_2O}–O_{H_2O})/2$. The molecular volumes of UO_2CO_3 and $UO_2(CO_3)_2^{2-}$ were calculated by extrapolation using the UO_2^{2+} and $UO_2(CO_3)_3^{4-}$ molecular volumes. The molecular volumes of the alkaline-earth uranyl carbonate species were obtained by adding the molecular volume of the tri-carbonate uranyl ion and that of the corresponding alkaline-earth cation as calculated from their fully hydrated radius. In each case, the molecular volume was used to calculate the equivalent spherical radius. Interestingly, Fig. 5 shows that the calculated diffusion coefficients display a general linear dependence on the inverse of the equivalent spherical radius with a R^2 value of approximately 0.93. Therefore, although the SE models fail to quantitatively predict the computed self-diffusion coefficient values, the molecular dynamics simulations indicate that when considering the entire family of uranyl carbonate species a general linear dependence on the equivalent spherical hydrated radius emerges as would be expected based on the SE models. Finally, although there is a clear decrease in diffusion coefficient when alkaline-earth cations bind to the uranyl tri-carbonate complex, the differences between the different alkaline-earth species are within uncertainties, an observation which suggests that a single value may be conveniently used in microscopic diffusion models for all alkaline-earth uranyl tri-carbonate species in bulk aqueous solutions.

4. CONCLUSIONS

Molecular dynamics simulations of alkaline-earth uranyl carbonate species in water were carried out to investigate a series of structural and dynamical hydration properties. In particular, the self-diffusion coefficients of these species were calculated in an effort to develop species-based uranyl diffusion models and thereby provide insight into uranyl reactive transport in subsurface environments.

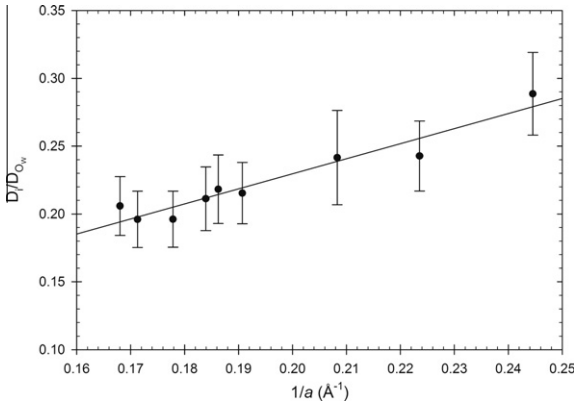

Fig. 5. Relative self-diffusion coefficients of the alkaline-earth uranyl carbonate species as a function of the inverse of the equivalent spherical radius.

Mean interatomic distances and coordination numbers were first compared with available ab initio and experimental data. Overall, the potential model gave a good description of the structural properties of the various aqueous species and in particular of the bidendate binding configuration adopted by calcium in the calcium uranyl tri-carbonate complexes. The MD simulations predict that the structure of the magnesium and strontium uranyl tri-carbonate complexes, for which no structural data is yet available, is similar to that of the calcium uranyl carbonate complexes, although magnesium may also adopt a monodentate binding configuration.

Interestingly, comparison with published experimental and theoretical studies as well as our molecular dynamics simulations indicates that a commonly used value of the diffusion coefficient of the uranyl ion (Brown et al., 1954a) does not correspond to the true limiting diffusion coefficient. The low value obtained by Brown et al. (1954a) could be due to the fact that their data were corrected for the presence of hydrogen ions only and not for the presence of other possible ions. Our calculated diffusion coefficient for the uranyl ion is, however, consistent with previous experimental studies (Kern and Orlemann, 1949; Brown et al., 1954b; Marx and Bischoff, 1976; Awakura et al., 1987) and the theoretical work of Mauerhofer et al. (2004).

Finally, the dynamics of water exchange around the alkaline-earth cations showed that the uranyl tri-carbonate molecule can impose a particular geometry on the cation's first hydration shell. Moreover, the water exchange kinetics around the alkaline-earth cation are affected differently depending on whether the imposed geometry matches or not the geometry of the fully hydrated species. As a result, the alkaline-earth uranyl carbonate complexes have distinct water exchange dynamics, which may lead to different reactivities.

ACKNOWLEDGMENTS

This research was supported by the US Department of Energy (DOE) through the Environmental Remediation Science Program (ERSP) of the Office of Biological and Environmental Research

(BER). The computer simulations were performed in part using the Molecular Science Computing Facility (MSCF) in the William R. Wiley Environmental Molecular Sciences Laboratory (EMSL), a national scientific user facility sponsored by the US DOE's Office of Biological and Environmental Research (OBER) and located at Pacific Northwest National Laboratory (PNNL). PNNL is operated for the DOE by Battelle Memorial Institute under Contract DE-AC05-76RL01830.

APPENDIX A. SUPPLEMENTARY DATA

Supplementary data associated with this article can be found, in the online version, at doi:10.1016/j.gca.2010.06.007.

REFERENCES

Viscosity of liquids. In *CRC Handbook of Chemistry and Physics*, 90th Ed. (ed. L. R. Lide). Taylor and Francis Group, Boca Raton, FL, pp. 175–179, Section 6.

Åberg M., Ferri D., Glaser J. and Grenthe I. (1983) Structure of the hydrated dioxouranium(VI) ion in aqueous solution. An X-ray diffraction and ^{1}H NMR study. *Inorg. Chem.* **22**, 3986–3989.

Albright J. N. (1972) X-ray diffraction studies of aqueous alkaline-earth chloride solutions. *J. Chem. Phys.* **56**, 3783–3786.

Allen P. G., Bucher J. J., Shuh D. K., Edelstein N. M. and Reich T. (1997) Investigation of aquo and chloro complexes of UO_2^{2+}, NpO_2^{+}, Np^{4+}, and Pu^{3+} by X-ray absorption fine structure spectroscopy. *Inorg. Chem.* **36**, 4676–4683.

Archer T. D., Birse S. E. A., Dove M. T., Redfern S. A. T., Gale J. D. and Cygan R. T. (2003) An interatomic potential model for carbonates allowing for polarization effects. *Phys. Chem. Miner.* **30**, 416–424.

Austin J. P., Sundararajan M., Vincent M. A. and Hillier I. H. (2009) The geometric structures, vibration frequencies and redox properties of the actinyl coordination complexes ($[AnO_2(L)_n]^m$; An = U, Pu, Np; L = H_2O, Cl^-, CO_3^{2-}, $CH_3CO_2^-$, OH^-) in aqueous solution, studied by density functional theory methods. *Dalton Trans.*, 5902–5909.

Awakura Y., Sato K., Majima H. and Hirono S. (1987) The measurement of the diffusion coefficient of U(VI) in aqueous uranyl sulfate solutions. *Metall. Trans. B* **18**, 19–23.

Axe L., Bunker G. B., Anderson P. R. and Tyson T. A. (1998) An XAFS analysis of strontium at the hydrous ferric oxide surface. *J. Colloid Interface Sci.* **199**, 44–52.

Bai J., Liu C. X. and Ball W. P. (2009) Study of sorption-restarted U(VI) diffusion in Hanford silt/clay material. *Environ. Sci. Technol.* **43**, 7706–7711.

Bargar J. R., Reitmeyer R. and Davis J. A. (1999) Spectroscopic confirmation of uranium(VI)–carbonato adsorption complexes on hematite. *Environ. Sci. Technol.* **33**, 2481–2484.

Berendsen H. J. C., Grigera J. R. and Straatsma T. P. (1987) The missing term in effective pair potentials. *J. Phys. Chem.* **91**, 6269–6271.

Bernhard G., Geipel G., Brendler V. and Nitsche H. (1996) Speciation of uranium in seepage waters of a mine tailing pile studied by time-resolved laser-induced fluorescence spectroscopy (TRLFS). *Radiochim. Acta* **74**, 87–91.

Bernhard G., Geipel G., Reich T., Brendler V., Amayri S. and Nitsche H. (2001) Uranyl(VI) carbonate complex formation: validation of the $Ca_2UO_2(CO_3)_3$(aq.) species. *Radiochim. Acta* **89**, 511–518.

Bleuzen A., Pittet P. A., Helm L. and Merbach A. E. (1997) Water exchange on magnesium(II) in aqueous solution: a variable temperature and pressure ^{17}O NMR study. *Magn. Reson. Chem.* **35**, 765–773.

Bourg I. C. and Sposito G. (2007) Molecular dynamics simulations of kinetic isotope fractionation during the diffusion of ionic species in liquid water. *Geochim. Cosmochim. Acta* **71**, 5583–5589.

Bourg I. C., Richter F. M., Christensen J. N. and Sposito G. (2010) Isotopic mass dependence of metal cation diffusion coefficients in liquid water. *Geochim. Cosmochim. Acta* **74**, 2249–2256.

Braithwaite A., Livens F. R., Richardson S., Howe M. T. and Goulding K. W. T. (1997) Kinetically controlled release of uranium from soils. *Eur. J. Soil Sci.* **48**, 661–673.

Brown R. D., Bunger W. B., Marshall W. L. and Secoy C. H. (1954a) The electrical conductivity of uranyl fluoride in aqueous solution. *J. Am. Chem. Soc.* **76**, 1580–1581.

Brown R. D., Bunger W. B., Marshall W. L. and Secoy C. H. (1954b) The electrical conductivity of uranyl sulfate in aqueous solution. *J. Am. Chem. Soc.* **76**, 1532–1535.

Bruneval F., Donadio D. and Parrinello M. (2007) Molecular dynamics study of the solvation of calcium carbonate in water. *J. Phys. Chem. B* **111**, 12219–12227.

Bühl M., Diss R. and Wipff G. (2005) Coordination environment of aqueous uranyl(VI) ion. *J. Am. Chem. Soc.* **127**, 13506–13507.

Bühl M. and Kabrede H. (2006) Mechanism of water exchange in aqueous uranyl(VI) ion. A density functional molecular dynamics study. *Inorg. Chem.* **45**, 3834–3836.

Bühl M., Kabrede H., Diss R. and Wipff G. (2006) Effect of hydration on coordination properties of uranyl(VI) complexes. A first-principles molecular dynamics study. *J. Am. Chem. Soc.* **128**, 6357–6368.

Caminiti R., Licheri G., Piccaluga G. and Pinna G. (1977) X-ray diffraction study of a "three-ion" aqueous solution. *Chem. Phys. Lett.* **47**, 275–278.

Caminiti R., Licheri G., Piccaluga G. and Pinna G. (1979) Diffraction of X-rays and hydration phenomena in aqueous solutions of $Mg(NO_3)_2$. *Chem. Phys. Lett.* **61**, 45–49.

Catti M., Pavese A. and Price G. D. (1993) Thermodynamics properties of $CaCO_3$ calcite and aragonite: a quasi-harmonic calculation. *Phys. Chem. Miner.* **19**, 472–479.

Chaillou G., Anschutz P., Lavaux G., Schäfer J. and Blanc G. (2002) The distribution of Mo, U, and Cd in relation to major redox species in muddy sediments of the Bay of Biscay. *Mar. Chem.* **80**, 41–59.

Chaillou G., Schäfer J., Blanc G. and Anschutz P. (2008) Mobility of Mo, U, As, and Sb within modern turbidites. *Mar. Geol.* **254**, 171–179.

Chialvo A. A. and Simonson J. M. (2003) The structure of $CaCl_2$ aqueous solutions over a wide range of concentration. Interpretation of diffraction experiments via molecular simulation. *J. Chem. Phys.* **119**, 8052–8061.

Chisholm-Brause C. J., Conradson S. D., Buscher C. T., Eller P. G. and Morris D. E. (1994) Speciation of uranyl sorbed at multiple binding sites on montmorillonite. *Geochim. Cosmochim. Acta* **58**, 3625–3631.

Clark D. L., Conradson S. D., Donohoe R. J., Keogh D. W., Morris D. E., Palmer P. D., Rogers R. D. and Tait C. D. (1999) Chemical speciation of the uranyl ion under highly alkaline conditions. Synthesis, structures, and oxo ligand exchange dynamics. *Inorg. Chem.* **38**, 1456–1466.

D'Angelo P., Nolting H.-F. and Pavel N. V. (1996) Evidence for multielectron resonances at the Sr *K* edge. *Phys. Rev. A* **53**, 798–805.

de Leeuw N. H. and Parker S. C. (1997) Atomistic simulation of the effect of molecular adsorption of water on the surface structure and energies of calcite surfaces. *Faraday Trans.* **93**, 467–475.

de Leeuw N. H. and Parker S. C. (2000) Modeling absorption and segregation of magnesium and cadmium ions to calcite surfaces: introducing $MgCO_3$ and $CdCO_3$ potential models. *J. Chem. Phys.* **112**, 4326–4333.

de Leeuw N. H. (2002) Molecular dynamics simulations of the growth inhibition effect of Fe^{2+}, Mg^{2+}, Cd^{2+}, and Sr^{2+} on calcite crystal growth. *J. Phys. Chem. B* **106**, 5241–5249.

Docrat T. I., Mosselmans J. F. W., Charnock J. M., Whiteley M. W., Collison D., Livens F. R., Jones C. and Edmiston M. J. (1999) X-ray absorption spectroscopy of tricarbonatodioxouranate(V), $[UO_2(CO_3)_3]^{5-}$, in aqueous solution. *Inorg. Chem.* **38**, 1879–1882.

Dong W. and Brooks S. C. (2006) Determination of the formation constants of ternary complexes of uranyl and carbonate with alkaline earth metals (Mg^{2+}, Ca^{2+}, Sr^{2+}, and Ba^{2+}) using anion exchange method. *Environ. Sci. Technol.* **40**, 4689–4695.

Dong W. and Brooks S. C. (2008) Formation of aqueous $MgUO_2(CO_3)_3^{2-}$ complex and uranium anion exchange mechanism onto an exchange resin. *Environ. Sci. Technol.* **42**, 1979–1983.

Dorosh A. K. and Skryshevskii A. F. (1965) The structural characteristics of the immediate environment of cations in aqueous solutions. *J. Struct. Chem.* **5**, 842–844.

Dove M. T., Winkler B., Leslie M., Harris M. J. and Salje E. K. (1992) A new interatomic potential model for calcite: applications to lattice dynamics studies, phase transition, and isotope fractionation. *Am. Miner.* **77**, 244–250.

Druchok M., Bryk T. and Holovko M. (2005) A molecular dynamics study of uranyl hydration. *J. Mol. Liq.* **120**, 11–14.

Dünweg B. and Kremer K. (1991) Microscopic verification of dynamic scaling in dilute polymer solutions: a molecular-dynamics simulation. *Phys. Rev. Lett.* **66**, 2996–2999.

Dünweg B. and Kremer K. (1993) Molecular dynamics simulation of a polymer chain in solution. *J. Chem. Phys.* **99**, 6983–6997.

Elzinga E. J., Tait C. D., Reeder R. J., Rector K. D., Donohoe R. J. and Morris D. E. (2004) Spectroscopic investigation of U(VI) sorption at the calcite–water interface. *Geochim. Cosmochim. Acta* **68**, 2437–2448.

Ewald P. P. (1921) Die Berechnung optischer und elektrostatischer Gitterpotentiale. *Ann. Phys.* **64**, 253–287.

Farkas I., Bányai I., Szabó Z. and Grenthe I. (2000) Rates and mechanisms of water exchange of UO_2^{2+}(aq) and UO_2(oxalate)$F(H_2O)^{2-}$: a variable-temperature ^{17}O and ^{19}F NMR study. *Inorg. Chem.* **39**, 799–805.

Fisler D. K., Gale J. D. and Cygan R. T. (2000) A shell model for the simulation of rhombohedral carbonate minerals and their point defects. *Am. Miner.* **85**, 217–224.

Frick R. J., Hofer T. S., Pribil A. B., Randolf B. R. and Rode B. M. (2009) Structure and dynamics of the UO_2^{2+} ion in aqueous solution: an ab initio QMCF MD study. *J. Phys. Chem. A* **113**, 12496–12503.

Fulton J. L., Heald S. M., Badyal Y. S. and Simonson J. M. (2003) Understanding the effects of concentration on the solvation structure of Ca^{2+} in aqueous solution. I: the perspective on local structure from EXAFS and XANES. *J. Phys. Chem. A* **107**, 4688–4696.

Gagliardi L., Grenthe I. and Roos B. J. (2001) A theoretical study of the structure of tricarbonatodioxouranate. *Inorg. Chem.* **40**, 2976–2978.

Geipel G., Amayri S. and Bernhard G. (2008) Mixed complexes of alkaline earth uranyl carbonates: a laser-induced time resolved fluorescence spectroscopic study. *Spectrochim. Acta* **71**, 53–58.

Greathouse J. A., O'Brien R. J., Bemis G. and Pabalan R. T. (2002) Molecular dynamics study of aqueous uranyl interactions with quartz (0 1 0). *J. Phys. Chem. B* **106**, 1646–1655.

Greathouse J. A. and Cygan R. T. (2005) Molecular dynamics simulation of uranyl(VI) adsorption equilibria onto an external montmorillonite surface. *Phys. Chem. Chem. Phys.* **7**, 3580–3586.

Greathouse J. A. and Cygan R. T. (2006) Water structure and aqueous uranyl(VI) adsorption equilibria onto external surfaces of beidellite, montmorillonite, and pyrophyllite: results from molecular simulations. *Environ. Sci. Technol.* **40**, 3865–3871.

Guilbaud P. and Wipff G. (1993) Hydration of UO_2^{2+} cation and its NO_3^- and 18-crown-6 adducts studied by molecular-dynamics simulations. *J. Phys. Chem.* **97**, 5685–5692.

Guilbaud P. and Wipff G. (1996) Force field representation of the UO_2^{2+} cation from free energy MD simulations in water. Tests on its 18-crown-6 and NO_3^- adducts, and on its calix[6]arene(6-) and CMPO complexes. *J. Mol. Struct. (THEOCHEM)* **366**, 55–63.

Guillaumont R., Fanghanel T., Fuger J., Grenthe I., Neck V., Palmer D. A. and Rand M. H. (2003) *Update on the Chemical Thermodynamics of Uranium, Neptunium, Plutonium, Americium and Technetium*. Elsevier, Amsterdam, Netherlands.

Harris D. J., Brodholt J. P. and Sherman D. M. (2003) Hydratin of Sr^{2+} in hydrothermal solutions from ab initio molecular dynamics. *J. Phys. Chem. B* **107**, 9056–9058.

Helm L. and Merbach A. E. (2005) Inorganic and bioinorganic solvent exchange mechanisms. *Chem. Rev.* **105**, 1923–1959.

Hemmingsen L., Amara P., Ansoborlo E. and Field M. J. (2000) Importance of charge transfer an polarization effects for the modeling of uranyl-cation complexes. *J. Phys. Chem. A* **104**, 4095–4101.

Hennig C., Tutschku J., Rossberg A., Bernhard G. and Scheinost A. C. (2005) Comparative EXAFS investigation of uranium(VI) and -(IV) aquo chloro complexes in solution using a newly developed spectroelectrochemical cell. *Inorg. Chem.* **44**, 6655–6661.

Hess B. (2002) Determining the shear viscosity of model liquids from molecular dynamics simulations. *J. Chem. Phys.* **116**, 209–217.

Hewish N. A., Neilson G. W. and Enderby J. E. (1982) Environment of Ca^{2+} ions in aqueous solvent. *Nature* **297**, 138–139.

Hofer T. S., Tran H. T., Schwenk C. F. and Rode B. M. (2004) Characterization of dynamics and reactivities of solvated ions by *ab initio* simulations. *J. Comput. Chem.* **25**, 211–217.

Hofer T. S., Randolf B. R. and Rode B. M. (2006) Sr(II) in water: a labile hydrate with a highly mobile structure. *J. Phys. Chem. B* **110**, 20409–20417.

Hoover W. G. (1985) Canonical dynamics – equilibrium phase-space distributions. *Phys. Rev. A* **31**, 1695–1697.

Ikeda A., Hennig C., Tsushima S., Takao K., Ikeda Y., Scheinost A. C. and Bernhard G. (2007a) Comparative study of uranyl(VI) and -(V) carbonato complexes in an aqueous solution. *Inorg. Chem.* **46**, 4212–4219.

Ikeda T., Boero M. and Terakura K. (2007b) Hydration properties of magnesium and calcium ions from constrained first principles molecular dynamics. *J. Chem. Phys.* **127**, 074503.

Ilton E. S., Qafoku N. P., Liu C., Moore D. A. and Zachara J. M. (2008) Advective removal of intraparticle uranium from contaminated vadose zone sediments, Hanford, U.S.. *Environ. Sci. Technol.* **42**, 1565–1571.

Impey R. W., Madden P. A. and McDonald I. R. (1983) Hydration and mobility of ions in solution. *J. Phys. Chem. B* **87**, 5071–5083.

Jorgensen W. L., Chandrasekhar J., Madura J. D., Impey R. W. and Klein M. L. (1983) Comparison of simple potential

functions for simulating liquid water. *J. Chem. Phys.* **79**, 926–935.

Kalinichev A. G. and Kirkpatrick R. J. (2002) Molecular dynamics modeling of chloride binding to the surfaces of calcium hydroxide, hydrated calcium aluminate, and calcium silicate phases. *Chem. Mater.* **14**, 3539–3549.

Kalinichev A. G., Wang J. and Kirkpatrick R. J. (2007) Molecular dynamics modeling of the structure, dynamics and energetics of mineral–water interfaces: application to cement materials. *Cem. Concr. Res.* **37**, 337–347.

Kalmykov S. N. and Choppin G. R. (2000) Mixed $Ca^{2+}/UO_2^{2+}/CO_3^{2-}$ complex formation at different ionic strengths. *Radiochim. Acta* **88**, 603–606.

Kelly S. D., Kemner K. M., Brooks S. C., Fredrickson J. K., Carroll S. L., Kennedy D. W., Zachara J. M., Plymale A. E. and Fendorf S. (2005) Ca–UO_2–CO_3 complexation – implications for bioremediation of U(VI). *Phys. Scr.* **T115**, 915–917.

Kelly S. D., Kemner K. M. and Brooks S. C. (2007) X-ray absorption spectroscopy identifies calcium–uranyl–carbonate complexes at environmental concentrations. *Geochim. Cosmochim. Acta* **71**, 821–834.

Kerisit S. and Parker S. C. (2004) Free energy of adsorption of water and metal ions on the {10.4} calcite surface. *J. Am. Chem. Soc.* **126**, 10152–10161.

Kerisit S., Cooke D. J., Spagnoli D. and Parker S. C. (2005) Molecular dynamics simulations of the interaction between water and inorganic solids. *J. Mater. Chem.* **15**, 1454–1462.

Kerisit S., Liu C. and Ilton E. S. (2008) Molecular dynamics simulations of the orthoclase (0 0 1)- and (0 1 0)-water interfaces. *Geochim. Cosmochim. Acta* **72**, 1481–1497.

Kerisit S. and Liu C. (2009) Molecular simulations of water and ion diffusion in nanosized mineral fractures. *Environ. Sci. Technol.* **43**, 777–782.

Kern D. M. H. and Orlemann E. F. (1949) The potential of the uranium(V), uranium(VI), couple and the kinetics of uranium(V) disproportionation in perchlorate media. *J. Am. Chem. Soc.* **71**, 2102–2106.

Koneshan S., Rasaiah J. C., Lynden-Bell R. M. and Lee H. (1998) Solvent structure, dynamics, and ion mobility in aqueous solutions at 25 °C. *J. Phys. Chem. B* **102**, 4193–4204.

Kruse W. and Taube H. (1961) Exchange and isomerization rates of complex ions of the aquo-bis-(ethylenediamine)-cobalt(III) series. *J. Am. Chem. Soc.* **83**, 1280–1284.

Kubicki J. D., Halada G. P., Jha P. and Phillips B. L. (2009) Quantum mechanical calculation of aqueous uranium complexes: carbonate, phosphate, organic and biomolecular species. *Chem. Cent. J.* **3**, 10.

Kumar P. P., Kalinichev A. G. and Kirkpatrick R. J. (2009) Hydrogen-bonding structure and dynamics of aqueous carbonate species from Car-Parrinello molecular dynamics simulations. *J. Phys. Chem. B* **113**, 794–802.

Laage D. and Hynes J. T. (2008) On the residence time for water in a solute hydration shell: application to aqueous halide solutions. *J. Phys. Chem. B* **112**, 7697–7701.

Lee S. H. and Rasaiah J. C. (1994) Molecular dynamics simulation of ionic mobility. I. Alkali metal cations in water at 25 °C. *J. Chem. Phys.* **101**, 6964–6974.

Lee S. H. and Rasaiah J. C. (1996) Molecular dynamics simulation of ion mobility. 2. Alkali metal and halide ions using the SPC/E model for water at 25 °C. *J. Phys. Chem.* **100**, 1420–1425.

Leung K., Nielsen I. M. B. and Kurtz I. (2007) Ab initio molecular dynamics study of carbon dioxide and bicarbonate hydration and the nucleophilic attack of hydroxide on CO_2. *J. Phys. Chem. B* **111**, 4453–4459.

Li Y.-H. and Gregory S. (1974) Diffusion of ions in sea water and in deep-sea sediments. *Geochim. Cosmochim. Acta* **38**, 703–714.

Licheri G., Piccaluga G. and Pinna G. (1976) X-ray diffraction study of the average solute species in $CaCl_2$ aqueous solutions. *J. Chem. Phys.* **64**, 2437–2441.

Lightstone F. C., Schwegler E., Hood R. Q., Gygi F. and Galli G. (2001) A first principles molecular dynamics simulation of the hydrated magnesium ion. *Chem. Phys. Lett.* **343**, 549–555.

Lightstone F. C., Schwegler E., Allesch M., Gygi F. and Galli G. (2005) A first-principles molecular dynamics study of calcium in water. *ChemPhysChem* **6**, 1745–1749.

Lins R. D., Vorpagel E. R., Guglielmi M. and Straatsma T. P. (2008) Computer simulation of uranyl uptake by the rough lipopolysaccharide membrane of *Pseudomonas aeruginosa*. *Biomacromolecules* **9**, 29–35.

Liu C., Zachara J. M., Qafoku O., McKinley J. P., Heald S. M. and Wang Z. (2004) Dissolution of uranyl microprecipitates in subsurface sediments at Hanford Site, USA. *Geochim. Cosmochim. Acta* **68**, 4519–4537.

Liu C., Jeon B.-H., Zachara J. M., Wang Z., Dohnalkova A. and Fredrickson J. K. (2006a) Kinetics of microbial reduction of solid phase U(VI). *Environ. Sci. Technol.* **40**, 6260–6296.

Liu C., Zachara J. M., Yantasee W., Majors P. D. and McKinley J. P. (2006b) Microscopic reactive diffusion of uranium in the contaminated sediments at Hanford, United States. *Water Resour. Res.* **42**, W12420.

Liu C., Zachara J. M., Qafoku N. P. and Wang Z. (2008) Scale-dependent desorption of uranium from contaminated subsurface sediments. *Water Resour. Res.* **44**, W08413.

Liu C., Shi Z. and Zachara J. M. (2009a) Kinetics of uranium(VI) desorption from contaminated sediments: effect of geochemical conditions and model evaluation. *Environ. Sci. Technol.* **43**, 6560–6566.

Liu C., Zachara J. M., Zhong L., Heald S. M., Wang Z., Jeon B.-H. and Fredrickson J. K. (2009b) Microbial reduction of intragrain U(VI) in contaminated sediment. *Environ. Sci. Technol.* **43**, 4928–4933.

Maigut J., Meier R., Zahl A. and Van Eldik R. (2008) Triggering water exchange mechanisms via chelate architecture. Shielding of transition metal centers by aminopolycarboxylate spectator ligands. *J. Am. Chem. Soc.* **130**, 14556–14569.

Majumdar D., Roszak S., Balasubramanian K. and Nitsche H. (2003) Theoretical study of aqueous uranyl carbonate (UO_2CO_3) and its hydrated complexes: $UO_2CO_3{\cdot}nH_2O$ ($n = 1$–3). *Chem. Phys. Lett.* **372**, 232–241.

Majumdar D. and Balasubramanian K. (2005) Theoretical studies on the electronic structures of $UO_2(CO_3)_2^{2-}$ and its metal salts: $M_2UO_2(CO_3)_2$ ($M = Li^+$ and Na^+). *Mol. Phys.* **103**, 931–938.

Marry V., Rotenberg B. and Turq P. (2008) Structure and dynamics of water at a clay surface from molecular dynamics simulation. *Phys. Chem. Chem. Phys.* **10**, 4802–4813.

Marx G. and Bischoff H. (1976) Transport processes of actinides in electrolyte solutions. I. Determination of ionic mobilities of uranium in aqueous solutions at 25 °C by the radioisotope method. *J. Radioanal. Chem.* **30**, 567–581.

Mason C. F. V., Turney W. R. J. R., Thomson B. M., Lu N. L., Longmire P. A. and Chisholm-Brause C. J. (1997) Carbonate leaching of uranium from contaminated soils. *Environ. Sci. Technol.* **31**, 2707–2711.

Mauerhofer E., Zhernosekov K. and Rösch F. (2004) Limiting transport properties and hydration numbers of actinyl ions in pure water. *Radiochim. Acta* **92**, 5–10.

McKinley J. P., Zachara J. M., Liu C. X., Heald S. C., Prenitzer B. I. and Kempshall B. W. (2006) Microscale controls on the fate of contaminant uranium in the vadose zone, Hanford Site, Washington. *Geochim. Cosmochim. Acta* **70**, 1873–1887.

McManus J., Berelson W. M., Klinkhammer G. P., Hammond D. E. and Holm C. (2005) Authigenic uranium: relationship to

oxygen penetration depth and organic carbon rain. *Geochim. Cosmochim. Acta* **69**, 95–108.

Megyes T., Grósz T., Radnai T., Bakó I. and Pálinkás G. (2004) Solvation of calcium ion in polar solvents: an X-ray diffraction an ab initio study. *J. Phys. Chem. A* **108**, 7261–7271.

Megyes T., Bakó I., Bálint S., Grósz T. and Radnai T. (2006) Ion pairing in aqueous calcium chloride solution: molecular dynamics simulation and diffraction studies. *J. Mol. Liq.* **129**, 63–74.

Melchionna S., Ciccotti G. and Holian B. L. (1993) Hoover NPT dynamics for systems varying in shape and size. *Mol. Phys.* **78**, 533–544.

Mills R. (1973) Self-diffusion in normal and heavy water in the range 1–40. *J. Phys. Chem.* **77**, 685–688.

Møller K. B., Rey R., Masia M. and Hynes J. T. (2005) On the coupling between molecular diffusion and solvation shell exchange. *J. Chem. Phys.* **122**, 114508.

Moreau G., Helm L., Purans J. and Merbach A. E. (2002) Structural investigation of the aqueous Eu^{2+} ion: comparison with Sr^{2+} using the XAFS technique. *J. Phys. Chem. A* **106**, 3034–3043.

Naor M. N., Nostrand K. V. and Dellago C. (2003) Car-Parrinello molecular dynamics simulation of the calcium ion in liquid water. *Chem. Phys. Lett.* **369**, 159–164.

Neely J. and Connick R. (1970) Rate of water exchange from hydrated magnesium ion. *J. Am. Chem. Soc.* **92**, 3476–3478.

Neuefeind J., Soderholm L. and Skanthakumar S. (2004) Experimental coordination environment of uranyl(VI) in aqueous solution. *J. Phys. Chem. A* **108**, 2733–2739.

Nichols P., Bylaska E. J., Schenter G. K. and de Jong W. (2008) Equatorial and apical solvent shells of the UO_2^{2+} ion. *J. Chem. Phys.* **128**, 124507.

Northrop J. H. and Anson M. L. (1929) A method for the determination of diffusion constants and the calculation of the radius and weight of the hemoglobin molecule. *J. Gen. Physiol.* **12**, 543–554.

O'Day P. A., Newville M., Neuhoff P. S., Sahai N. and Carroll S. A. (2000) X-ray absorption spectroscopy of strontium(II) coordination. *J. Colloid Interface Sci.* **222**, 184–197.

Ohtaki H. and Radnai T. (1993) Structure and dynamics of hydrated ions. *Chem. Rev.* **93**, 1157–1204.

Parkman R. H., Charnock J. M., Livens F. R. and Vaughan D. J. (1998) A study of the interaction of strontium ions in aqueous solution with the surfaces of calcite and kaolinite. *Geochim. Cosmochim. Acta* **62**, 1481–1492.

Pavese A., Catti M., Price G. D. and Jackson R. A. (1992) Interatomic potentials for $CaCO_3$ polymorphs (calcite and aragonite), fitted to elastic and vibrational data. *Phys. Chem. Miner.* **19**, 80–87.

Pavese A., Catti M., Parker S. C. and Wall A. (1996) Modelling of the thermal dependence of structural and elastic properties of calcite, $CaCO_3$. *Phys. Chem. Miner.* **23**, 89–93.

Pfund D. M., Darab J. G., Fulton J. L. and Ma Y. (1994) An EXAFS study of strontium ions and krypton in supercritical water. *J. Phys. Chem. A* **98**, 13102–13107.

Phillips B. L., Casey W. H. and Neugebauer Crawford S. (1997a) Solvent exchange in $AlF_x(H_2O)_{6-x}^{3-x}$(aq) complexes: ligand-directed labialization of water as an analogue for ligand-induced dissolution of oxide minerals. *Geochim. Cosmochim. Acta* **61**, 3041–3049.

Phillips B. L., Neugebauer Crawford S. and Casey W. H. (1997b) Rate of water exchange between $Al(C_2O_4)(H_2O)_4^+$(aq) complexes and aqueous solutions determined by ^{17}O-NMR spectroscopy. *Geochim. Cosmochim. Acta* **61**, 4965–4973.

Phillips B. L., Tossell J. A. and Casey W. H. (1998) Experimental and theoretical treatment of elementary ligand exchange reactions in aluminum complexes. *Environ. Sci. Technol.* **32**, 2865–2870.

Predota M., Cummings P. T. and Wesolowski D. J. (2007) Electric double layer at the rutile (1 1 0) surface. 3. Inhomogeneous viscosity and diffusivity measurement by computer simulations. *J. Phys. Chem. C* **111**, 3071–3079.

Pyykkö P., Li J. and Runeberg N. (1994) Quasirelativistic pseudopotential study of species isoelectronic to uranyl and the equatorial coordination of uranyl. *J. Phys. Chem.* **98**, 4809–4813.

Rotenberg B., Marry V., Vuilleumier R., Malikova N., Simon C. and Turq P. (2007) Water and ions in clays: unraveling the interlayer/micropore exchange using molecular dynamics. *Geochim. Cosmochim. Acta* **71**, 5089–5101.

Rotzinger F. P. (2007) The water-exchange mechanism of the $[UO_2(OH_2)_5]^{2+}$ ion revisited: the importance of a proper treatment of electron correlation. *Chem. Eur. J.* **13**, 800–811.

Rustad J. R., Nelmes S. L., Jackson V. E. and Dixon D. A. (2008) Quantum-chemical calculations of carbon-isotope fractionation in CO_2(g), aqueous carbonate species, and carbonate minerals. *J. Phys. Chem. A* **113**, 542–555.

Ryckaert J. P., Ciccotti G. and Berendsen H. J. C. (1977) Numerical-integration of cartesian equations of motion of a system with constraints – molecular-dynamics of *n*-alkanes. *J. Comput. Phys.* **23**, 327–341.

Ryss A. I. and Radchenko I. V. (1965) An X-ray diffraction study of aqueous solutions of magnesium tetrafluoroborate. *J. Struct. Chem.* **6**, 422–423.

Sakuma H., Tsuchiya T., Kawamura K. and Otsuki K. (2004) Local behavior of water molecules on brucite, talc, and halite surfaces: a molecular dynamics study. *Mol. Simul.* **30**, 861–871.

Sakuma H. and Kawamura K. (2009) Structure and dynamics of water on muscovite mica surfaces. *Geochim. Cosmochim. Acta* **73**, 4100–4110.

Salmon P. S., Howells W. S. and Mills R. (1987) The dynamics of water molecules in ionic solution: II. Quasi-elastic neutron scattering and tracer diffusion studies of the proton and ion dynamics in concentrated Ni^{2+}, Cu^{2+} and Nd^{3+} aqueous solutions. *J. Phys. C Solid State Phys.* **20**, 5727–5747.

Schneppensieper T., Seibig S., Zahl A., Tregloan P. and Van Eldik R. (2001) Influence of chelate effects on the water-exchange mechanism of polyaminecarboxylate complexes of iron(III). *Inorg. Chem.* **40**, 3670–3676.

Schwenk C. F., Loeffler H. H. and Rode B. M. (2001) Molecular dynamics simulations of Ca^{2+} in water: comparison of a classical simulation including three-body corrections and Born–Oppenheimer ab initio and density functional theory quantum mechanical/molecular mechanics simulations. *J. Chem. Phys.* **115**, 10808–10813.

Sémon L., Boehme C., Billard I., Hennig C., Lützenkirchen K., Reich T., Roßberg A. and Rossini I. W. G. (2001) Do perchlorate and triflate anions bind to the uranyl cation in an acidic aqueous medium? A combined EXAFS and quantum mechanical investigation. *ChemPhysChem* **2**, 591–598.

Seward T. M., Henderson C. M. B., Charnock J. M. and Driesner T. (1999) An EXAFS study of solvation and ion pairing in aqueous strontium solutions to 300 °C. *Geochim. Cosmochim. Acta* **63**, 2409–2418.

Smith W., and Forester T. R. (1996) DL_POLY is a package of molecular simulation routines. Copyright The Council for the Central Laboratory of the Research Councils, Daresbury Laboratory at Daresbury, Nr. Warrington.

Steele H. M., Wright K., Nygren M. A. and Hillier I. H. (2000) Interaction of the (0 0 1) surface of muscovite with Cu(II), Zn(II), and Cd(II): a computer simulation study. *Geochim. Cosmochim. Acta* **64**, 257–262.

Stejskal E. O. and Tanner J. E. (1965) Spin diffusion measurements: spin echoes in the presence of a time-dependent field gradient. *J. Chem. Phys.* **42**, 288–292.

Stubbs J. E., Veblen L. A., Elbert D. C., Zachara J. M., Davis J. A. and Veblen D. R. (2009) Newly recognized hosts for uranium in the Hanford Site vadose zone. *Geochim. Cosmochim. Acta* **73**, 1563–1576.

Swarzenski P. W. and Baskaran M. (2007) Uranium distribution in the coastal waters and pore waters of Tampa Bay, Florida. *Mar. Chem.* **104**, 43–57.

Szabó Z., Glaser J. and Grenthe I. (1996) Kinetics of ligand exchange reactions for uranyl(2+) fluoride complexes in aqueous solution. *Inorg. Chem.* **35**, 2036–2044.

Thompson H. A., Brown, Jr., G. E. and Parks G. A. (1997) XAFS spectroscopic study of uranyl coordination in solids an aqueous solution. *Am. Miner.* **82**, 483–496.

Todorova T., Hünenberg P. H. and Hutter J. (2008) Car-Parrinello molecular dynamics simulations of $CaCl_2$ aqueous solutions. *J. Chem. Theory Comput.* **4**, 779–789.

Tongraar A. and Rode B. M. (2005) Ab initio QM/MM dynamics of anion–water hydrogen bonds in aqueous solution. *Chem. Phys. Lett.* **403**, 319–341.

Tsushima S., Uchida Y. and Reich T. (2002) A theoretical study on the structures of $UO_2(CO_3)_3^{4-}$, $Ca_2UO_2(CO_3)_3^0$, and $Ba_2UO_2(CO_3)_3^0$. *Chem. Phys. Lett.* **357**, 73–77.

Vallet V., Wahlgren U., Schimmelpfennig B., Szabó Z. and Grenthe I. (2001) The mechanism of water exchange in $[UO_2(H_2O)_5]^{2+}$ and $[UO_2(oxalate)_2(H_2O)]^{2-}$, as studied by quantum chemical methods. *J. Am. Chem. Soc.* **123**, 11999–12008.

Vanysek P. (2010) Ionic conductivity and diffusion at infinite dilution. In *CRC Handbook of Chemistry and Physics* (ed. D. R. Lide), 90th ed. Taylor and Francis Group, Boca Raton, FL, pp. 76–78, Section 5.

Vásquez J., Boo C., Poblet J. M., de Pablo J. and Bruno J. (2003) DFT studies of uranyl acetate, carbonate, and malonate, complexes in solution. *Inorg. Chem.* **42**, 6136–6141.

Wahlgren U., Moll H., Grenthe I., Schimmelpfennig B., Maron L., Vallet V. and Gropen O. (1999) Structure of uranium(VI) in strong alkaline solutions. A combined theoretical and experimental investigation. *J. Phys. Chem. A* **103**, 8257–8264.

Wåhlin P., Danilo C., Vallet V., Réal F., Flament J. P. and Wahlgren U. (2008) An investigation of the accuracy of different DFT functionals on the water exchange reaction in hydrated uranyl(VI) in the ground state and first excited state. *J. Chem. Theory Comput.* **4**, 569–577.

Wander M. C. F., Kerisit S., Rosso K. M. and Schoonen M. A. A. (2006) Kinetics of triscarbonato uranyl reduction by aqueous ferrous iron: a theoretical study. *J. Phys. Chem. A* **110**, 9691–9701.

Wang J., Kalinichev A. G. and Kirkpatrick R. J. (2006) Effects of substrate structure and composition on the structure dynamics, and energetics of water at mineral surfaces: a molecular dynamics modeling study. *Geochim. Cosmochim. Acta* **70**, 562–582.

Wang Z., Zachara J. M., Yantasee W., Gassman P. L., Liu C. and Joly A. G. (2004) Cryogenic laser induced fluorescence characterization of U(VI) in Hanford vadose zone pore waters. *Environ. Sci. Technol.* **38**, 5591–5597.

Yeh I. C. and Hummer G. (2004) System-size dependence of diffusion coefficients and viscosities from molecular dynamics simulations with periodic boundary conditions. *J. Phys. Chem. A* **108**, 15873–15879.

Zheng Y., Anderson R. F., Van Geen A. and Fleisher M. Q. (2002) Remobilization of authigenic uranium in marine sediments by bioturbation. *Geochim. Cosmochim. Acta* **66**, 1759–1772.

Associate editor: William H. Casey